C. R. Physique 19 (2018) 533–542

Contents lists available at ScienceDirect

Comptes Rendus Physique

www.sciencedirect.com

Physics and arts / Physique et arts

Cultural heritage investigations using cosmic muons

Utilisation des muons cosmiques dans le domaine des biens culturels

Sara Vanini [a,*], Fabio Ambrosino [d,e], Lorenzo Bonechi [g], Germano Bonomi [c], Paolo Checchia [b], Raffaello D'Alessandro [f,g], Giancarlo Nebbia [b], Giulio Saracino [d,e], Aldo Zenoni [c], Gianni Zumerle [b]

[a] *University of Padova, via Marzolo 8, 35131 Padova, Italy*
[b] *INFN Sezione di Padova, via Marzolo 8, 35131 Padova, Italy*
[c] *University of Brescia, via Branze 38, 25123 Brescia, Italy*
[d] *University of Napoli, Via Cinthia, 80126 Fuorigrotta, NA, Italy*
[e] *INFN Sezione di Napoli, Strada Comunale Cintia, 80126 Napoli, Italy*
[f] *University of Firenze, via G. Sansone, 1, 50019 Sesto Fiorentino, FI, Italy*
[g] *INFN Sezione di Firenze, Via Giovanni Sansone, 1, 50019 Sesto Fiorentino, FI, Italy*

ARTICLE INFO

Article history:
Available online 23 August 2018

Keywords:
Cosmic rays
Cultural heritage
Muon tomography
Muon radiography
Image reconstruction

Mots-clés :
Rayons cosmiques
Patrimoine culturel
Tomographie muons
Radiographie muons
Imagerie

ABSTRACT

Cosmic rays are a constant, free source of radiation that can be exploited in various ways to probe heavy and extended objects. Analyzed with proper detection systems, they can produce radiographic as well as tomographic images of bulky materials. Several applications have been proposed, in particular in the domain of security checks, and some are presently fielded for routine use. In this paper, cosmic muon technology is presented, and its possible use in the field of cultural heritage is described.

RÉSUMÉ

Les rayons cosmiques représentent une source constante et gratuite de radiation qui peut être utilisée de différentes façons pour sonder des objets massifs et volumineux. Analysés avec des systèmes de détection spécialisés, ils peuvent produire aussi bien des images radiographiques que des images tomographiques d'objets de grandes dimensions. De nombreuses applications ont été proposées, dont quelques-unes sont actuellement utilisées, notamment dans le domaine de la sécurité. Ce papier présente la technologie des muons cosmiques et décrit des utilisations possibles dans le domaine des biens culturels.

* Corresponding author.
E-mail address: sara.vanini@pd.infn.it (S. Vanini).

https://doi.org/10.1016/j.crhy.2018.08.002
1631-0705/

1. Introduction

As techniques in physics progressed and improved along the years, several methodologies developed in this field have been applied to investigations, both for historical and conservative purposes, in different areas of cultural heritage. Among these, a number of techniques involving the use of atomic or nuclear radiation such as α-particle backscattering, X-ray radiography, X-ray fluorescence, Particle-Induced X-ray Emission (PIXE), Particle-Induced Gamma-ray Emission (PIGE), and many others. All of these methods imply the use either of radiation sources (natural and/or electronic) or of particle accelerators. Such sources need a rather complex procedure in order to ensure the safety of the operating personnel as well as the safety of the objects under investigation, often precious if not unique. In some instances though, it is possible to exploit the largest source of natural radiation freely available: the universe. Cosmic radiations of different natures (mainly protons) are in fact constantly falling on Earth through the atmosphere, producing particle cascades whose most abundant products, at sea level, are muons (μ). Cosmic muons are rather energetic charged particles that can penetrate deeply in different kinds of materials and in the Earth's crust itself. One can take advantage of these characteristics to produce radiographic images of very large objects of various nature, in particular human artifacts such as historical buildings, caves etc. Modern technologies mainly related to high-energy physics experiments have provided sophisticated tools to detect muons with high efficiency and high precision, thus allowing one to produce precise radiographic as well as tomographic (3D) images of the object traversed by cosmic muons. The obvious advantage of such a technique is the completely safe operation, since cosmic radiation is always present on Earth and no additional radiation is produced. This also means that this technique is totally noninvasive. Last but not least, cosmic muons are a free source, therefore no expenses for the construction of artificial sources (or accelerators) need to be budgeted, and only costs related to the detection systems have to be considered. Section 2 of this paper will describe two different ways of using cosmic muons in order to produce images of massive objects, namely the absorption method and the Muon Scattering Tomography (MST) method. Section 3 is dedicated to the technical description of the absorption method, while section 5 will describe the rather sophisticated reconstruction technique of the MST method. Sections 4, 6, and 7 will show some examples of the various methods applied to some cases of interest in the field of cultural heritage.

2. The method

Muons are charged particles almost identical to electrons, but about 200 times heavier. Like electrons, they do not have nuclear charge and, therefore, they cannot undergo nuclear interactions. They are relatively long living (about 100 microseconds on average in the Earth's rest frame) and highly penetrating. Hitting the Earth's surface with a rate of about 100 $s^{-1}\cdot m^{-2}$, their energy spectrum is peaked slightly below 1 GeV, with a high-energy tail, and their flux goes approximately as $\cos^2\zeta$, where ζ is the zenith angle. This means that muon intensity is maximum near the zenith at any position on the Earth's surface.

The high penetration of cosmic-ray muons can be used to explore dense and inaccessible volumes. The first known application was in 1955 [1] and it was aimed at determining the depth of the rock layer above an underground tunnel. The first known application to cultural heritage was proposed by Nobel Prize laureate L.W. Alvarez to inspect the Chefren pyramid, searching for hollow vaults [2]. Recently, very interesting findings in a different pyramid have been published [3], as reported in Section 4. Furthermore, several volcano inspections were performed in order to characterize the magmatic chambers [4]. In all such cases, cosmic muons are used as ordinary X-rays in radiography by looking at their absorption pattern.

A completely different approach, based on multiple Coulomb scattering (MCS), is the so-called muon scattering tomography (MST) proposed in 2003 [5]. Charged particles as muons are deflected and slowed down by crossing a target volume. Measuring the deviation angles allows one to obtain information about the radiation length (or its inverse, the Linear Scattering Density LSD $\lambda = 1/X_0$) of an unknown material.

The two approaches on the use of cosmic muons, namely the absorption evaluation and the MST, require a different experimental setup and, consequently, they can be applied to extremely different situations: the former requires a single detector located in general below or on the side of the volume to investigate, the latter needs two detectors to measure the position and the direction of the muons both when they enter the volume to be inspected and when they exit. Absorption can be applied to the investigation of very large objects (volcanoes, mines, buildings, etc.). On the other hand, in order to obtain a tomographic reconstruction with MST, the collected muon sample must include a wide angular span and hence the distance between the two detectors must be of the order of their own dimensions. Therefore, MST can be an adequate tool to investigate the content of volumes not too large with respect to the reasonable dimensions of the detectors and, considering in particular cultural heritage applications, not exceeding a few meters such as small vaults in buildings, sarcophaguses, or any other thick and heavy object whose contents are not readily reachable. While the absorption technique has been used in the field of cultural heritage, the applications of MST are insofar bound to safety and security issues (see a few examples in the section below and in Ref. [6]). Nevertheless, MST is a rather sophisticated and powerful technique, and applications to the historical and artistic patrimony could be foreseen.

3. Reconstruction techniques for absorption analysis

The conceptual scheme of muon absorption analysis is simple and immediate, given its similarity to standard X-ray imaging. However, there are some important differences and peculiarities, which have to be accounted for in order to obtain an image of the target by means of its muon absorption pattern.

In ordinary X-ray imaging, the object of the radiography is placed close to the detector and is illuminated by an almost uniform flux of incoming X-rays orthogonal to the plane of the image. It is thus sufficient to detect, on a sensitive surface (e.g., the X-ray film), the flux of surviving radiation in order to obtain an image of the object under scrutiny. The function describing the transmitted flux $T(x, y)$ in a point of the X-ray film plane will carry information on the overall density along the straight line orthogonal to the plane of the image and passing through the point (x, y): the direction of the incoming X-rays is known (along z in this example), and its intensity is also known and uniform.

In muon absorption, the detector itself is typically much smaller than the object under scrutiny (so that in most cases it can be considered to be point like) and is placed quite far from it, typically tens to hundreds of meters away: in this case, the information about the density is not carried by the transmission as a function of the position (x, y) on the image plane, since each point of the detector surface is actually crossed by radiation coming from the whole target. It is thus mandatory to measure the *direction* (ζ, φ) of the incoming muons, so that the transmission $T(\zeta, \varphi)$ (i.e. the ratio of transmitted flux to incoming flux) will carry information on the integrated density of the target along the direction (ζ, φ) from the (point-like) detector. As a consequence, the detector cannot simply measure the passage of the muon, but it must also measure its direction with good accuracy, i.e. it must be a *tracking* detector. Since the muons' energy spectrum changes as a function of ζ, the variation must be taken into account in the absorption analysis since the measured flux of muons N^{μ} as a function of (ζ, φ) must be compared to the incoming flux $F(\zeta, \varphi)$ to obtain the transmission, which will in turn depend on the integrated density ρ along the path of the muon:

$$T(\zeta, \varphi) = \frac{N^{\mu}(\zeta, \varphi)}{F(\zeta, \varphi)} \tag{1}$$

$F(\zeta, \varphi)$ here represents the number of muons that are expected to reach the detector in the absence of obstacles along their path: it can be either estimated by means of simulations using empirical models of the muon flux reaching the Earth, or measured directly by pointing the detector at regions of "free sky".

The integrated flux of muons observed by the detector $N^{\mu}(\zeta, \varphi)$ carries the information on $\rho_{\zeta\varphi} s_{\zeta\varphi}$, i.e. the product of the average density $\rho_{\zeta\varphi}$ and the path length $s_{\zeta\varphi}$ that the muon has to cross along the (ζ, φ) direction to reach the detector. The absorption caused by the presence of the object under muographic scrutiny will reduce the transmission to values lower than one: the transmission is actually a measurement of the probability for muons traveling along a given direction to cross the target material without being absorbed along their path. This probability depends on the energy of the incoming muon and on the average density of the target times its overall thickness (i.e. on $\rho_{\zeta\varphi} s_{\zeta\varphi}$). Simulations of the muon energy spectrum and of its interaction with the target material, and the knowledge of the total thickness of the target (e.g., via Digital Terrain Models) allow one to simulate the expected transmission along the direction (ζ, φ) for any hypothesized average density $\rho_{\zeta\varphi}$. This is usually done assuming as a starting point a reasonable density value for the given muographic target, and then adjusting it to match the observed transmission. Local anomalies in density (e.g., underground cavities, or magma conduits in volcanoes) can thus be detected and located with a good spatial resolution: an empty volume, such as a hidden chamber in a large structure, will show up as a localized angular region with measured transmission significantly higher than expected (see Eq. (1); see also Mt. Echia example, later in the text).

As in conventional radiography, images taken from different points of view may be combined to extract a three-dimensional tomography of the target: this can be done either by placing several detectors simultaneously around the target at the same time or by changing the position of the detector and performing measurements from different positions.

A detector for muon absorption analysis has to be sensitive to the passage of a muon and must detect its direction with good angular resolution, typically a few tens of mrad or better. This is usually done by assembling several planes of xy-position sensitive detectors, placed at some distance from each other in order to form a so-called "muon telescope". While two planes provide the minimal configuration in order to measure the direction of incoming muons, typically three or more planes are adopted to provide redundant precision on the determination of the muon direction.

According to the need and to the morphology of the target and of the measurement site, different solutions may be adopted for the detector technology. A first family of detectors (*electronic detectors*) is based on the conversion of the energy released by the interaction of the muon with the device into an electronic signal. These detectors usually require low electric power (e.g., solar panels and/or batteries), therefore they are well adapted to field use. Electronic detectors offer the possibility to analyze data in real time. Contrary to an X-ray film, they may be reused as many times as required, in different places and conditions. Another family of devices is known as *emulsion detectors*. These devices are very similar to conventional X-ray films. They do not require power and, given the excellent spatial resolution, the two detection planes may be placed rather close to each other, still having the required angular sensitivity, thus providing a rather compact device. They are thus well suited for situations where very compact detectors are needed, and in all situations where no electric power is available. On the other hand, they do not provide online information and the process of offline data analysis is complex. Indeed, sophisticated automatic microscopy scanning tools are needed, usually requiring several weeks to scan

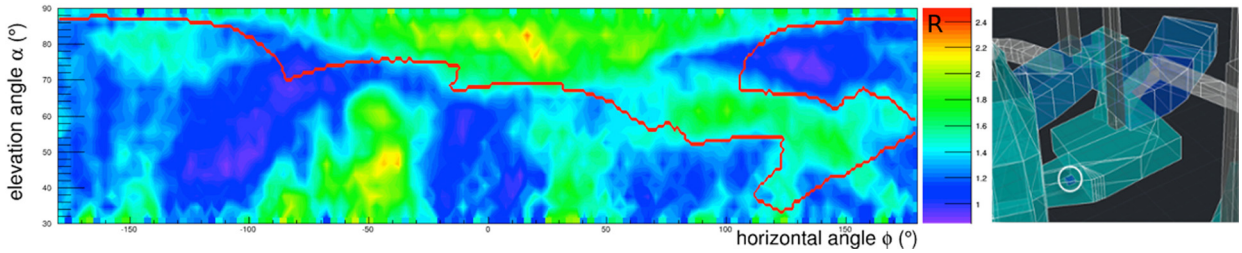

Fig. 1. Left: muon radiography image of the cavities in Mt. Echia. Right: 3D image of the room (showed in blue) as seen from the detector. The position of the detector is visible as a small blue box inside the white circle.

Fig. 1. À gauche : image par radiographie muons des cavités du mont Echia. À droite : image de la chambre (en bleu) du point de vue du détecteur. La position du détecteur est représentée par le petit carré bleu à l'intérieur du cercle blanc.

each m^2 of exposed emulsion film with current state-of-the-art technologies. However, new technologies being developed will likely reduce this time by orders of magnitude in the next future, see [7]. Nuclear emulsion films are not reusable.

4. Possible applications of the absorption analysis

Muon absorption is suitable to map density anomalies in very large objects, such as the top part of volcano inner structures and lava domes [8–11]. The technique has been successfully applied or proposed for a variety of applications, ranging from mining [12] to archeology [13], including tunnel searches [14], geological surveys [15,16], nuclear waste [17–20], and reactor monitoring [21,22].

Two very recent results deserve particular interest. The success of muon absorption in underground imaging has been recently verified [14], with the observation of known cavities excavated over the centuries in the yellow tuff of Monte Echia, the site of the earliest settlement of the city of Naples (Italy) in the 8th century BC. An electronic detector was used to demonstrate, for the first time, the capability to find relatively small (a few meters) cavities under a rock overburden of about 40 m. The interaction of incoming muons with the rather complex structure of the underground edifices was simulated in order to compare the expected and measured transmission. The largest structures appeared after a few hours of measurement. After 26 days of data taking, the whole system of known cavities had shown up in the transmission pattern, and the comparison with the expectation also allowed one to obtain the indication of an unknown cavity showing up as a region with higher than expected transmission. Fig. 1 shows a schematic view of the underground structures. The plot on the left shows the R variable as a function of the elevation and horizontal angles. R is defined as the ratio between the flux of muons measured under the mountain and the expected one, in the hypothesis that no cavities are present. If no voids are crossed by muons, R is close to 1 (blue color in the plot), while voids are observed as regions with $R > 1$ (green–yellow colors in the plot). The red line corresponds to the shape of the expected muon radiography image of the room, shown in blue on the right panel, as seen from the detector. The position of the detector is visible as a small blue box. The other green signals on the left panel correspond to other known cavities, except for two signals that have been interpreted as unknown voids.

More recently, Morishima, et al. [3] reported the discovery of a large unknown void inside the Cheops pyramid. A big void (at least 30 m in length) has been detected using the techniques described in Section 3. Emulsion films placed in the Queen's chamber integrated muon data for several months. Later, two different types of electronic detectors (a scintillator-based detector in the Queen's chamber and a gas-based detector placed outside the pyramid) confirmed the finding. The pyramid side view with a sketch of the interior structure and the discovered big void are shown in Fig. 2.

This spectacular result confirms, almost 50 years later, the validity of the intuition of L. Alvarez in searching for vaults in pyramids using muon absorption analysis and paves the road for further applications of this noninvasive technique in the exploration of archeological heritage sites.

5. Reconstruction techniques for muon scattering tomography

The measurement of muon deviation due to MCS can be used to produce 3-dimensional images of the material distribution inside dense objects. As discussed in the introduction, this method requires to measure the position and the direction of the particles at the entrance as well as at the exit of the volume to be inspected. The deviation angle, projected on a plane containing the initial muon direction, has a distribution approximately Gaussian for particles of the same momentum, with zero mean and a root-mean-square, which is a function of the muon momentum p, of the material's thickness X, and of the radiation length X_0 [23] according to the formula:

$$\sigma \approx \frac{13.6\ (\mathrm{MeV})}{p\,c}\sqrt{\frac{X}{X_0}} \tag{2}$$

were c is the speed of light.

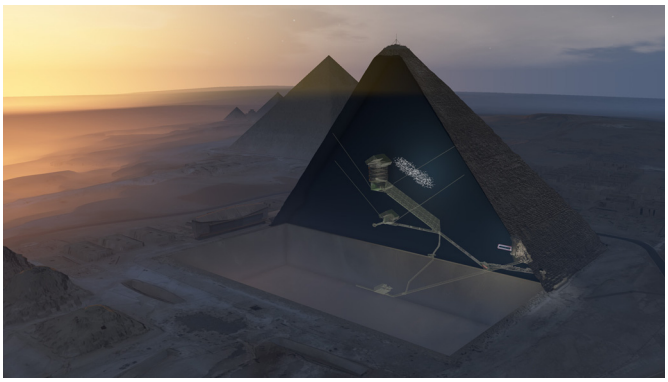

Fig. 2. Side view of the Cheops pyramid. King's and Queen's chambers are sketched in the center of the pyramid, connected by the Grand Gallery. The cosmic muon sensors are positioned under the Queen's chamber and outside the pyramid facing the North Face corridor. The Big Void discovered using muon imaging has a cross-section similar to that of the Grand Gallery and a minimum length of 30 m. It is situated above the Grand Gallery, as shown in the picture. Picture courtesy of ScanPyramids Mission.

Fig. 2. Vue latérale de la pyramide de Khéops. Les chambres du roi et de la reine sont dessinées au centre de la pyramide, et elles sont connectées par la grande galerie. Les détecteurs des muons sont positionnés sous la chambre de la reine et aussi en dehors de la pyramide, en face du couloir nord. Le grand creux découvert par l'imagerie muons présente une section proche de celle de la grande galerie et une longueur minimum de 30 m. Il est situé en dessus de la grande galerie, comme indiqué sur la figure. Avec l'aimable autorisation de ScanPyramids Mission.

If the muon sample is not monochromatic, the same relation holds replacing $1/p$ with $1/p_{\text{average}} = \sqrt{< 1/p^2 >}$. The value assigned to this quantity, usually not known with great precision, affects the overall density scale of the reconstructed image. The presence of known objects in the reconstructed space can help fix the scale [24].

All the different reconstruction methods divide the space between detectors in volume elements, called voxels, in which the object material is assumed to be homogeneous. The simplest reconstruction method assumes that the scattering of any individual muon occurs in a single point, which coincides with the Point of Closest Approach (PoCA) of the two straight lines measured by the detectors. A map of the LSD distribution can be obtained through computing for each voxel the standard deviation of the scattering angle of the muons for which the PoCA falls inside that voxel. From the standard deviation the voxel LSD can be computed using Eq. (2) with p_{average} replacing p_i. This method, computationally very fast, works well when in the reconstructed space few small objects are present with a much higher LSD than in the rest of the volume, otherwise it fails. A more powerful method is based on maximum likelihood expectation maximization (MLEM) [25], [26]. If the material is not homogeneous, the volume to be inspected is divided in N cubic cells, called voxels, where the LSD is assumed to be constant. For a muon i it is possible to write from Eq. (2)

$$\sigma_i^2 = \left(\frac{13.6\,(\text{MeV})}{p_i c}\right)^2 \Sigma_k L_{ik}\lambda_k \tag{3}$$

where λ_k is the LSD of voxel k and L_{ik} the crossing path of muon i in the same voxel. With a sample of M muons, assuming a Gaussian probability density function for the projected scattering angle:

$$P_i = P(\Delta\theta_i \mid \sigma_i) = \frac{1}{\sigma_i\sqrt{2\pi}} \mathrm{e}^{\Delta\theta_i^2/(2\sigma_i^2)} \tag{4}$$

the N unknowns $\{\lambda_k; k = 1...N\}$ can be related to M measurements $\{\Delta\theta_i^2; i = 1..M\}$ of the scattering angles $\Delta\theta_i$. A likelihood function can be written, whose maximization gives an estimate of the $\{\lambda_k\}$ values. If, as it is usually the case, the individual muon momenta are not known, the fixed p_{average} value previously defined is used in Eq. (3). The likelihood function can be modified to include the measurement of the so-called displacement, i.e. the distance between the exit point of each muon measured on the OUT detector and the exit point in the absence of scattering, extrapolated from the initial muon direction. See [25] for details. Given the large numbers occurring (M and N can be of the order of millions), an iterative procedure is necessary to maximize the log-likelihood functional and obtain reasonably approximate λ_k values.

Although performing, this method is quite complex and can be computationally very slow, so that several other algorithms have been proposed for tomographic reconstruction, e.g., [27,28].

The detectors for MST must have good angular and space precision over large areas. Moreover, they must guarantee stability in time and position. Candidate detectors for muon tomography are described in Refs. [29–34].

6. Possible applications of muon scattering tomography

The first application proposed [35] was addressed to detect heavy metals in transport containers, to contrast nuclear contraband. A portal based on drift tubes detectors has been realized and is in operation in Freeport (The Bahamas) [36].

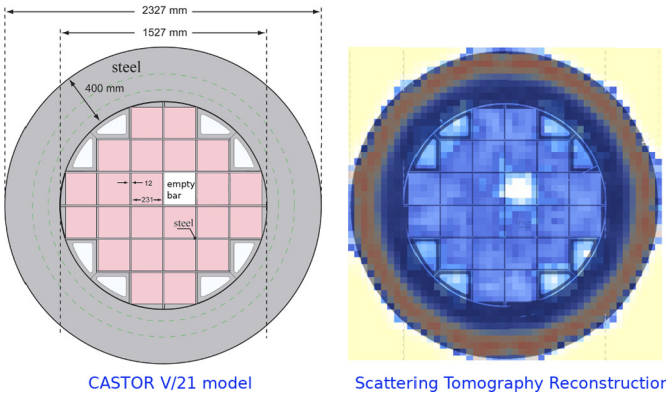

Fig. 3. CASTOR V/21 simulation model (left) and MST reconstruction (right). The reconstructed image has voxel area in the image plane of 5×5 cm^2 and uses muon data taken over 1 day. The sketch of the CASTOR section is superimposed on the reconstructed image on the right to show the expected position of the missing fuel bar.

Fig. 3. Simulation du Castor V/21 et reconstruction d'image avec MST. L'image obtenue a une dimension de voxel de 5×5 cm^2. Elle a été obtenue par une mesure acquise sur environ un jour. L'image à droite montre clairement l'absence d'un élément de combustible.

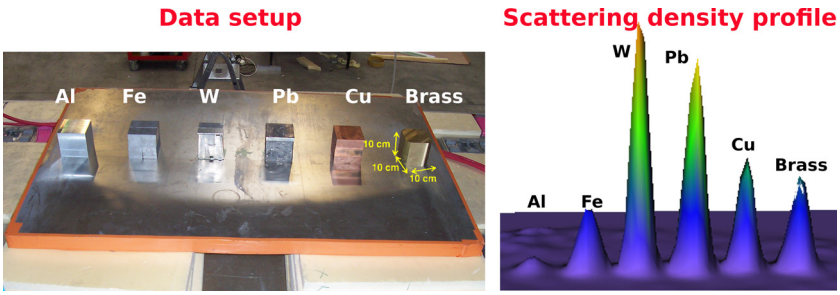

Fig. 4. Test performed at the Laboratori Nazionali di Legnaro (LNL) with cosmic muon data crossing different materials. Samples of different materials are inspected with the Scattering Tomography technique. Left: a photo shows the setup of the samples ready for data taking. Right: the image density profile obtained with MLEM reconstruction algorithm shows peaks representative of the different LSD values and thus of the different materials.

Fig. 4. Échantillons des différents matériaux mesurés avec la technique MST aux Laboratori Nazionali di Legnaro (LNL). À gauche : photo avec l'ensemble des échantillons. À droite : l'image du profil d'intensité obtenu par l'algorithme de reconstruction MLEM montre des pics qui représentent les différentes valeurs du paramètre LSD et donc des différents matériaux.

Another application concerns the detection of the so-called orphan sources, i.e. radioactive sources sometimes present in scrap metal transported to foundries. It can happen that radiation sources, well shielded by a heavy metal cask and by the scrap metal itself, are not detected by the radiation portals usually present at the foundry's entrance. In such cases, the source is melted inside the foundry with disastrous consequences for the plant and the public. It has been demonstrated that a dedicated MST portal can detect the heavy metal shield of the source in a short time, of the order of 5 min [37].

Another foreseen industrial application implies imaging of different components present in a blast furnace during operations (coke, burden, reduced metal). Results based on simulation of ideal detectors surrounding the whole furnace and of smaller, more realistic detectors, have shown the potentiality of the technology to map the internal distribution of the material [38]. On this application, other studies gave also interesting results [39,24,40–42].

Another promising field [17–20,43] is related to the inspection of dry storage containers for spent nuclear fuel. Simulation results about the detection of a missing bar in a CASTOR V/21 container are shown in Fig. 3. On the left, there is the sketch of a container with a missing bar, and on the right the average density along vertical axis, reconstructed using scattered muons information. The absence of a bar is clearly visible.

Interesting tests have been performed in order to assess the full potentiality of MST. Small samples of known materials were placed inside the inspected volume to test the capability of the technique to discriminate objects of different LSD [44]. Fig. 4 shows a picture of the samples on the left, and the LSD profile obtained with MLEM reconstruction algorithm on the right. A discussion about the accuracy and precision of the measurements of reconstructed LSD values versus the actual ones can be found in [24].

In order to test MST on a larger scale, a FIAT 500 car was positioned in the setup as shown in Fig. 5. One can recognize the main metal structures of the car like the wheel axis, the engine and in particular the high density/high atomic number battery. In the right part of the figure, a block of 1 liter of lead was positioned in the engine vault (bright red spot).

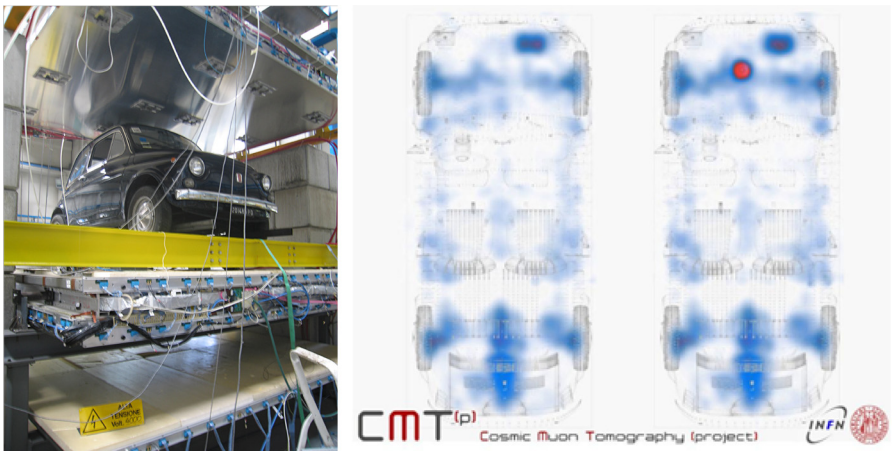

Fig. 5. Image of a small vehicle FIAT 500 at LNL. The car is placed in the inspected volume as shown in the picture on the left. The reconstructed image using a scattering tomography algorithm, on the right, clearly shows the main metal structures of the car, including a 1-liter lead block hidden in the engine vault, on the rightmost panel.

Fig. 5. Image d'une voiture FIAT 500 aux laboratoires LNL. La voiture a été placée à l'intérieur du volume d'inspection (photo de gauche). L'image reconstruite par l'algorithme tomographique (au centre) montre clairement les structures métalliques principales, y compris un bloc de plomb d'un litre caché dans le compartiment moteur à droite).

7. Control of building stability

Another technique exploiting cosmic ray muons, different from both the absorption and the MST techniques described above, has also been recently proposed for alignment measurement in large mechanical structure and for the monitoring of the stability of historical buildings [45,46]. In the latter application, since muons travel along almost straight lines and can easily cross floors and walls of buildings, they can effectively represent a suitable probe for stability monitoring. The suggested stability monitoring system is composed of two elements. The first one is a "muon telescope", composed of a set of three muon detector modules axially aligned at a relative distance of 50 cm. Each module is composed of two orthogonal layers of 120 scintillating optical fibers with 3 mm $\times$ 3 mm cross section and 400 mm length.

The two planes of orthogonal scintillating fibers provide the measurement of the crossing position of an incident muon, with a pitch of 3 mm. The expected spatial resolution on the hit coordinate is about 0.9 mm. The "muon telescope" is mechanically fixed to a structural element of the building constituting the reference system. Its axis is aligned in the direction corresponding to the part of the structure whose displacements should be monitored. The second element of the monitoring system is a single muon detector module, with the same geometry and structure as the previous ones, positioned as "muon target" on the point of the structure to be monitored. Thanks to their high penetrability, cosmic ray muons are able to easily cross all the building structures interposed between the two elements of the monitoring system, suffering only small deviations of their trajectories by multiple Coulomb scattering. In this way, it is possible to continuously monitor the horizontal displacements of the "muon target" relative to the "muon telescope". The detection of a relative displacement would imply a deformation of the building structure.

The expected performance of the proposed stability monitoring system has been studied in the realistic case of an historical building in the City of Brescia, namely the "Palazzo della Loggia" (see Fig. 6). The stability of the roof of the palace has been monitored for ten years through a conventional mechanical system based on the elongation of metallic wires, up to 25 m long, stretched between different points of the wooden structure of the roof. Seasonal deformations of the order of a few millimeters superimposed to a progressive collapse of about 1 mm per year of the structure of the roof were detected.

The relevant masonry structures of the "Palazzo della Loggia" building and the structure and composing materials of the "muon telescope" and "muon target" were modeled in a Monte Carlo code based on GEANT4, in order to predict the performance of the proposed stability monitoring system in the specific case study and compare it with the conventional mechanical system one.

In three specific simulations, the "muon telescope" and the "muon target" have been positioned one above the other at a different vertical distance ($\simeq$350 cm, $\simeq$880 cm, and $\simeq$1300 cm). The "muon telescope" was placed 300 cm below a 15-cm-thick wooden layer, simulating the ceiling of the "Salone Vanvitelliano" of the "Palazzo della Loggia", and the "muon target" on different positions on the roof structure.

In Fig. 7 the expected resolution of the measurement of the horizontal displacement between the "muon target" and the "muon telescope", as a function of the data taking time is plotted, for the three examined conditions, up to a data taking time of one month. The uncertainty in the measurement is mainly due to the statistics of the collected muons and it decreases increasing the measurement time.

Fig. 6. The "Palazzo della Loggia" of the town of Brescia (1574).

Fig. 6. Le « Palazzo della Loggia » à Brescia (Italie) (1574).

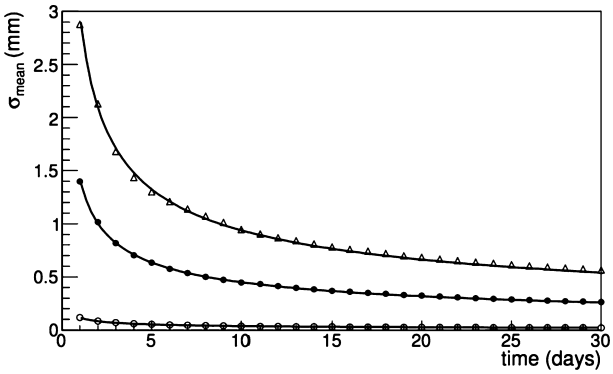

Fig. 7. Resolution of the measurement of the horizontal displacement between the "muon target" and the "muon telescope" as a function of the data taking time, in the three different configurations: (○), vertical distance of ≃350 cm, (●), vertical distance of ≃880 cm, and (△) vertical distance of ≃1300 cm.

Fig. 7. Relation entre l'incertitude standard de la valeur moyenne de la distribution des données et les temps d'acquisitions des données elles-mêmes pour le *trigger* des muons dans les positions P1 (○), P2 (●) et P3 (△).

For example, in one month of data taking, when "muon target" and "muon telescope" are positioned 13.0 m far apart, a measurement uncertainty of the order of 0.5 mm may be achieved. The same uncertainty may be achieved over a week of data taking when the vertical distance between them is around 8.8 m.

Typical time scales of progressive structural deformations in historical buildings may span over several years; therefore, the proposed stability-monitoring system based on cosmic ray muon detection seems to be suitable for such application. In addition, in spite of limitations in promptness, it may offer several advantages relative to conventional mechanical and optical systems: i) possibility to operate also when the parts of the building to be monitored are separated by masonry structures; ii) flexibility of installation inside the building structure; iii) little invasiveness, no structural modifications needed; iv) absence of moving mechanical parts and little maintenance; v) low sensitivity to environmental conditions; vi) use of a natural and ubiquitous, high-penetrating radiation.

8. Conclusions

Both cosmic ray radiography and tomography have been widely demonstrated. The advantage of disposing of a permanent, free source of highly penetrating radiation is obvious from a safety as well as from an economical point of view. The present detection technology opens the possibility to investigate large and bulky objects to unveil hidden structures and/or to characterize the contents of sealed human artifacts with a totally noninvasive procedure. While the absorption technique is simpler and allows the investigation of extremely large objects, MST must be confined to smaller volumes, but it offers the possibility of discriminating different material composing the inspected object with a good degree of resolution. Both

the described techniques represent a powerful tool that can be fruitfully used to investigate large artifacts of interest for archeology and for the cultural heritage in general.

References

[1] E. George, Cosmic rays measure overburden of tunnel, Commonw. Eng. 1955 (1955) 455–457.
[2] L.W. Alvarez, et al., Search for hidden chambers in the pyramids, Science 167 (1970) 832–839, https://doi.org/10.1126/science.167.3919.832.
[3] K. Morishima, et al., Discovery of a big void in Khufu's pyramid by observation of cosmic-ray muons, Nature 552 (2017) 386, https://doi.org/10.1038/nature24647.
[4] K. Nagamine, et al., Method of probing inner-structure of geophysical substance with the horizontal cosmic-ray muons and possible application to volcanic eruption prediction, Nucl. Instrum. Methods Phys. Res., Sect. A, Accel. Spectrom. Detect. Assoc. Equip. 356 (2) (1995) 585–595, https://doi.org/10.1016/0168-9002(94)01169-9.
[5] K.R. Borozdin, et al., Surveillance: radiographic imaging with cosmic-ray muons, Nature 422 (2003) 277, https://doi.org/10.1038/422277a.
[6] P. Checchia, Review of possible applications of cosmic muon tomography, J. Instrum. 11 (12) (2016) C12072.
[7] M. Yoshimoto, et al., Hyper-track selector nuclear emulsion readout system aimed at scanning an area of one thousand square meters, Prog. Theor. Exp. Phys. 2017 (10) (2017) 103H01, https://doi.org/10.1093/ptep/ptx131.
[8] K. Jourde, et al., Effects of upward-going cosmic muons on density radiography of volcanoes, arXiv:1307.6758.
[9] J. Marteau, et al., Muons tomography applied to geosciences and volcanology, in: New Developments in Photodetection NDIP11, Nucl. Instrum. Methods Phys. Res., Sect. A, Accel. Spectrom. Detect. Assoc. Equip. 695 (2012) 23–28, https://doi.org/10.1016/j.nima.2011.11.061.
[10] A. Anastasio, et al., The MU-RAY detector for muon radiography of volcanoes, in: Vienna Conference on Instrumentation 2013, Nucl. Instrum. Methods Phys. Res., Sect. A, Accel. Spectrom. Detect. Assoc. Equip. 732 (2013) 423–426, https://doi.org/10.1016/j.nima.2013.05.159.
[11] D. Carbone, et al., An experiment of muon radiography at Mt. Etna (Italy), Geophys. J. Int. 196 (2) (2014) 633–643, https://doi.org/10.1093/gji/ggt403, http://arxiv.org/abs//oup/backfile/content_public/journal/gji/196/2/10.1093/gji/ggt403/2/ggt403.pdf.
[12] L. Malmqvist, et al., Theoretical studies of in-situ rock density determinations using underground cosmic-ray muon intensity measurements with application in mining geophysics, Geophysics 44 (9) (1979) 1549–1569, https://doi.org/10.1190/1.1441026.
[13] H. Gómez, et al., Studies on muon tomography for archaeological internal structures scanning, J. Phys. Conf. Ser. 718 (5) (2016) 052016.
[14] G. Saracino, et al., Imaging of underground cavities with cosmic-ray muons from observations at Mt. Echia (Naples), Sci. Rep. 7 (2017) 1181, https://doi.org/10.1038/s41598-017-01277-3.
[15] L.G. Dedenko, et al., Prospects of the study of geological structures by muon radiography based on emulsion track detectors, Bull. Lebedev Phys. Inst. 41 (8) (2014) 235–241, https://doi.org/10.3103/S1068335614080065.
[16] J. Klinger, et al., Simulation of muon radiography for monitoring CO_2 stored in a geological reservoir, Int. J. Greenh. Gas Control 42 (2015) 644–654, https://doi.org/10.1016/j.ijggc.2015.09.010.
[17] G. Jonkmans, et al., Nuclear waste imaging and spent fuel verification by muon tomography, Ann. Nucl. Energy 53 (2013) 267–273, https://doi.org/10.1016/j.anucene.2012.09.011.
[18] A. Clarkson, et al., Characterising encapsulated nuclear waste using cosmic-ray Muon Tomography (MT), in: 4th International Conference on Advancements in Nuclear Instrumentation Measurement Methods and their Applications, 2015, pp. 1–7, https://doi.org/10.1109/ANIMMA.2015.7465529.
[19] D. Poulson, et al., Cosmic ray muon computed tomography of spent nuclear fuel in dry storage casks, Nucl. Instrum. Methods Phys. Res., Sect. A, Accel. Spectrom. Detect. Assoc. Equip. 842 (2017) 48–53, https://doi.org/10.1016/j.nima.2016.10.040.
[20] S. Chatzidakis, C.K. Choi, L.H. Tsoukalas, Analysis of spent nuclear fuel imaging using multiple Coulomb scattering of cosmic muons, IEEE Trans. Nucl. Sci. 63 (6) (2016) 2866–2874, https://doi.org/10.1109/TNS.2016.2618009.
[21] K. Borozdin, et al., Cosmic ray radiography of the damaged cores of the Fukushima reactors, Phys. Rev. Lett. 109 (2012) 152501, https://doi.org/10.1103/PhysRevLett.109.152501.
[22] J. Perry, et al., Imaging a nuclear reactor using cosmic ray muons, J. Appl. Phys. 113 (2013) 184909, https://doi.org/10.1063/1.4804660.
[23] K.A. Olive, et al., Review of particle physics, Chin. Phys. C 38 (2014) 090001, https://doi.org/10.1088/1674-1137/38/9/090001.
[24] E. Aströn, et al., Precision measurements of linear scattering density using muon tomography, J. Instrum. 11 (07) (2016) P07010.
[25] L.J. Schultz, et al., Statistical reconstruction for cosmic ray muon tomography, IEEE Trans. Image Process. 16 (8) (2007) 1985–1993, https://doi.org/10.1109/TIP.2007.901239.
[26] M. Benettoni, et al., Noise reduction in muon tomography for detecting high density objects, J. Instrum. 8 (12) (2013) P12007.
[27] S. Xiao, et al., A modified multi-group model of angular and momentum distribution of cosmic ray muons for thickness measurement and material discrimination of slabs, Nucl. Sci. Tech. 29 (2) (2018) 28, https://doi.org/10.1007/s41365-018-0363-7.
[28] T.J.S. Lee, A. Foley, Novel precision enhancement algorithm with reduced image noise in cosmic muon tomography applications, Nucl. Technol. Radiat. Prot. 31 (2016) 51–64, https://doi.org/10.2298/NTRP1601051L.
[29] K. Gnanvo, et al., Detection and imaging of high-Z materials with a muon tomography station using GEM detectors, in: IEEE Nuclear Science Symposium & Medical Imaging Conference, 2010, pp. 552–559, https://doi.org/10.1109/NSSMIC.2010.5873822.
[30] X. Wang, et al., Design and construction of muon tomography facility based on MRPC detector for high-Z materials detection, in: IEEE Nuclear Science Symposium and Medical Imaging Conference Record (NSS/MIC), Anaheim, CA, 2012, pp. 83–85, https://doi.org/10.1109/NSSMIC.2012.6551065.
[31] G. Russo, et al., Strip detectors for a portal monitor application, J. Instrum. 9 (11) (2014) P11008.
[32] M. Biglietti, et al., Development of a novel micro pattern gaseous detector for cosmic ray muon tomography, in: Frontier Detectors for Frontier Physics: Proceedings of the 13th Pisa Meeting on Advanced Detectors, Pisa, Italy, 24–30 May 2015, Nucl. Instrum. Methods Phys. Res., Sect. A, Accel. Spectrom. Detect. Assoc. Equip. 824 (2016) 220–222, https://doi.org/10.1016/j.nima.2015.11.025.
[33] A. Nishio, et al., Development of nuclear emulsion detector for muon radiography, in: 26th International Conference on Nuclear Tracks in Solids (ICNTS26) Kobe, Japan, 15–19 September 2014, Phys. Proc. 80 (2015) 74–77, https://doi.org/10.1016/j.phpro.2015.11.084.
[34] A. Anastasio, et al., The MU-RAY detector for muon radiography of volcanoes, in: Vienna Conference on Instrumentation 2013, 11–15 February 2013, Nucl. Instrum. Methods Phys. Res., Sect. A, Accel. Spectrom. Detect. Assoc. Equip. 732 (2013) 423–426, https://doi.org/10.1016/j.nima.2013.05.159.
[35] W. Priedhorsky, et al., Detection of high-Z objects using multiple scattering of cosmic ray muons, Rev. Sci. Instrum. 74 (2003) 4294–4297, https://doi.org/10.1063/1.1606536.
[36] G. Blanpied, et al., Material discrimination using scattering and stopping of cosmic ray muons and electrons: differentiating heavier from lighter metals as well as low-atomic weight materials, in: Symposium on Radiation Measurements and Applications 2014 (SORMA XV), Nucl. Instrum. Methods Phys. Res., Sect. A, Accel. Spectrom. Detect. Assoc. Equip. 784 (2015) 352–358, https://doi.org/10.1016/j.nima.2014.11.027.
[37] Muons scanner to detect radioactive sources hidden in scrap metal containers (MU-STEEL), EU publications Research Fund for Coal and Steel RFSR-CT-2010-00033, https://doi.org/10.2777/75975.
[38] Study of the capability of muon tomography to map the material composition inside a blast furnace (MU-BLAST), EU Publications Research Fund for Coal and Steel RFSR-CT-2014-00027.

[39] H. Xianfeng, et al., Exploring the capability of muon scattering tomography for imaging the components in the blast furnace, ISIJ Int. 58 (1) (2018) 35–42, https://doi.org/10.2355/isijinternational.ISIJINT-2017-384.
[40] G. Nagamine, et al., Probing the inner structure of blast furnaces by cosmic-ray muon radiography, INIS 41.
[41] N.N.W.B. Gilboy, P.M. Jenneson, Industrial thickness gauging with cosmic-ray muons, in: Ananda Mohan Ghose Memorial Issue, Radiat. Phys. Chem. 74 (6) (2005) 454–458, https://doi.org/10.1016/j.radphyschem.2005.08.007.
[42] J. Sauerwald, et al., Investigation of the coke network and cohesive zone by muon tomography, Technical contribution to the 6th International Congress on the Science and Technology of Ironmaking ICST.
[43] P. Checchia, et al., Muon tomography for spent nuclear fuel control, ESARDA Bull. 54 (2017) 2.
[44] S. Pesente, et al., First results on material identification and imaging with a large-volume muon tomography prototype, Nucl. Instrum. Methods Phys. Res., Sect. A, Accel. Spectrom. Detect. Assoc. Equip. 604 (3) (2009) 738–746, https://doi.org/10.1016/j.nima.2009.03.017.
[45] I. Bodini, et al., Cosmic ray detection based measurement systems: a preliminary study, Meas. Sci. Technol. 18 (11) (2007) 3537.
[46] A. Donzella, Stability monitoring of a historical building by means of cosmic ray tracking, Nuovo Cimento 37C (2014) 223–232.